

Original Article

TNFRSF6 induces mitochondrial dysfunction and microglia activation in the in vivo and in vitro models of sepsis-associated encephalopathy

Danfeng Yu, Yanmei Ji, Jing Zhang, Xiaochuan Huang*

Department of Neurocritical Medicine, Taihe Hospital, Hubei University of Medicine, No. 32 Renmin South Road, Shiyuan City 442000, Hubei Province, China



Article Info

Abstract



Article history:

Received: December 18, 2023

Accepted: February 21, 2024

Published: March 31, 2024

Use your device to scan and read the article online



Sepsis-associated encephalopathy (SAE) is a serious complication of sepsis. The tumour necrosis factor receptor superfamily member 6 (TNFRSF6) gene encodes the Fas protein, and it participates in apoptosis induced in different cell types. This study aimed to explore TNFRSF6 function in SAE. The SAE mouse model was established by intraperitoneal injection of LPS in TNFRSF6^{-/-} mice and C57BL/6J mice. Microglia were treated with LPS to establish the cell model. The learning, memory and cognitive functions in mice were tested by behavioral tests. Nissl staining was utilized for determining neuronal injury. Microglial activation was tested by immunofluorescence assay. ELISA was utilized for determining TNF- α , IL-1 β , IL-6, and IL-10 contents. Mitochondrial dysfunction was measured by mitochondrial oxygen consumption, ATP content, ROS production, and JC-1 assay. TNFRSF6 was upregulated in the LPS-induced mouse model and cell model. TNFRSF6 deficiency notably alleviated the impaired learning, memory and cognitive functions in SAE mice. Furthermore, we found that TNFRSF6 deficiency could alleviate neuronal injury, microglial activation, and inflammation in SAE mice. Additionally, mitochondrial dysfunction in the SAE mice was improved by TNFRSF6 depletion. In the LPS-induced microglia, we also proved that TNFRSF6 knockdown reduced inflammatory response inhibited ROS production, and alleviated mitochondrial dysfunction. TNFRSF6 induced mitochondrial dysfunction and microglia activation in the in vivo and in vitro models of SAE.

Keywords: Sepsis-associated encephalopathy, TNFRSF6, Microglia activation, Mitochondrial dysfunction.

1. Introduction

Sepsis a disease with high lethality and morbidity, which is defined as life-threatening organ dysfunction caused by a dysregulated host response to infection [1]. The diffuse brain dysfunction caused by sepsis is known as sepsis-associated encephalopathy (SAE) and it is a serious complication of sepsis [2]. In accordance with reports, approximately 9-71% of severe sepsis patients experience SAE [3, 4]. The clinical symptoms of SAE include mental disorder, impaired memory, cognitive impairment, and deep coma [5]. After the acute phase of sepsis, these mental states persist for a long time, seriously affecting the patient's quality of life. SAE is associated with neuronal damage in the brain, mitochondrial dysfunction, disruption of the blood-brain barrier, and the development of neuroinflammation, which may impair learning, memory, and cognitive functions [5, 6]. However, SAE pathogenesis is still unclear. Therefore, exploring SAE pathogenesis can help develop new therapeutic targets and improve the life quality of patients.

Microglia are resident macrophages in the central nervous system (CNS), which are associated with the initiation and progression of neuroinflammatory reactions in SAE. Microglia activation is typically classified into the

pro-inflammatory neurotoxic (M1) phenotype and the anti-inflammatory (M2) phenotype [7]. When sepsis occurs, the activated microglia change into M1 phenotype to release inflammatory factors, reactive oxygen species (ROS), and neurotransmitters, thereby causing neuronal damage and impairing learning and memory ability [8]. Research have indicated microglia activation exerts a vital function in assorted neurodegenerative diseases, including Alzheimer's disease, stroke, and Parkinson's disease [9-11]. In addition, several evidence have confirmed that inhibiting the over-activation of microglia can improve SAE. For example, CB2R exerts a protective function against SAE via suppressing microglia activation and neuronal pyroptosis [12]. YY1 inhibits microglia M1 polarization to alleviate SAE progression [13]. Nevertheless, the detailed molecular mechanism of microglia activation in SAE needs to be further clarified.

The tumour necrosis factor receptor superfamily member 6 (TNFRSF6) gene encodes the Fas protein which can trigger apoptosis and be conducive to maintaining lymphocyte homeostasis and preventing autoimmunity [14]. Studies have indicated that TNFRSF6 is involved in the destruction of insulin-producing cells and accelerates the development of diabetes [15]. TNFRSF6 mutation can im-

* Corresponding author.

E-mail address: huangxiaochuan_edu@outlook.com (X. Huang).

Doi: <http://dx.doi.org/10.14715/cmb/2024.70.3.15>

pair apoptosis in a human autoimmune lymphoproliferative syndrome. It is reported that the levels of TNFRSF6 in the brain of Alzheimer's disease patients are elevated, and the interaction between TNFRSF6 and APOE4 is considered a genetic risk factor for sporadic Alzheimer's disease [16]. However, the function of TNFRSF6 in SAE remains unclear.

This study is aimed to investigate TNFRSF6 function in SAE and microglia activation, which may be conducive to revealing the SAE pathogenesis.

2. Material and methods

2.1. Cell culture

Primary mouse microglia (CP-M110; M-microglia) and human microglia (CP-H123; H-microglia) were obtained from Procell Life Science & Technology Co. Ltd. (Wuhan, China) and incubated in DMEM/F12 medium (CM-M110, Procell) added with FBS, penicillin, and streptomycin. Microglia were stimulated with 1 $\mu\text{g}/\text{ml}$ LPS (Sigma-Aldrich, USA) for 24 h to establish the cell model.

2.2. The establishment of SAE mouse model

TNFRSF6-knockout (TNFRSF6^{-/-}) mice were purchased from Taihe Hospital, Hubei University of Medicine. WT C57BL/6J mice (male, 4-month-old, 20–25 g) were obtained from Taihe Hospital, Hubei University of Medicine. All mice were kept at 22–24°C for one week of adaptive feeding. Animal experiments were approved by the Ethics Committee of Taihe Hospital, Hubei University of Medicine. WT mice and TNFRSF6^{-/-} mice were divided into the sham group (n=16) and the sepsis group (n=16). SAE mice were intraperitoneally injected with 10 mg/kg LPS dissolved in saline. The sham-operated mice received equal volumes of saline.

2.3. Behavioral tests

2.3.1. Barnes maze

After modeling, mice were performed with Barnes maze to determine their learning and memory [17]. We prepared a circular platform with 20 evenly spaced holes. One of the holes was connected to the target box. We placed the mice on the table and stimulated them to discover the target box through noise and light. The space acquisition phase lasts for a total of four days, with two experiments per day, each lasting for 3 minutes. The mice experienced a reference memory stage on the first and eighth days after training. During the formal experiment, we used the Any Maze video tracking system (SD Instruments, San Diego, CA) to record the latency to discover the target box.

2.3.2. Fear conditioning test

One day after the Barnes maze experiment, mice were performed with the fear conditioning test [18]. We placed the mice in the testing chamber two minutes in advance, and then mice were received with tone-foot shock pairings within 30 seconds. The tone (2000 Hz, 85 dB) lasted for 30 seconds, and foot shock (0.7 mA) only existed in the last 2 seconds. The next day, the mice were placed in the same chamber again and their freezing behavior was recorded for 6 minutes without any stimulation. Freezing is defined as a posture that is completely immobile except for breathing. Then mice were placed in another chamber and recorded their freezing behavior without tone stimulation for three minutes, followed by recording their freezing

behavior with tone stimulation for 4.5 minutes.

2.3.3. Novel object recognition test (NORT)

NORT was performed to evaluate recognition memory. We prepared a square field as an arena, where mice were placed to familiarize themselves with the environment for three minutes. In the formal experiment, we placed two identical objects on the field, allowing mice to explore for five minutes. After 24 h, we replaced one of the familiar objects with a new object that the mice had not come into contact with and allowed the mice to explore for five minutes. Then the preference index after the experiment was calculated.

2.3.4. Morris Water Maze (MWM) test

MWM consists of a circular steel pool with a diameter of 120 centimeters and a height of 60 centimeters, and a hidden platform with a diameter of 10 centimeters. We poured opaque water into the pool and kept the water temperature at 23 °C. The hidden platform was placed approximately 1 centimeter below the water surface. The mice were trained for four consecutive days before conducting formal experiments on the fifth day. During the training period, mice were randomly placed in different directions of the pool and allowed to locate the platform within one minute, and the latency to the platform was recorded. The mice that did not find the platform were guided to the platform for a 10-second rest. On the fifth day, we withdrew the platform and placed mice in the pool, recording the number of platform crossings within 60 seconds and the number of seconds to search for the platform.

2.4. Nissl staining

After 48 h of modeling, mice were anesthetized and then subjected to transcardiac perfusion with 4% paraformaldehyde. Then, brains were removed and fixed by 4% paraformaldehyde and embedded in paraffin at 4 °C for a whole night. Brain sections were cut into 4 μm . Next, sections were stained with 0.1% cresyl violet acetate (Sigma) and then dehydrated by ethanol, followed by clearing with xylene. After that, sections were observed through a microscope (Olympus, Tokyo, Japan).

2.5. Immunofluorescence (IF) assay

The paraffin-embedded brain sections were deparaffinized, rehydrated, and boiled in Tris-EDTA solution (Beyotime) for half an hour for antigen recovery. Next, sections were blocked with 5% goat serum and cultured with primary antibody against Iba-1 (Santa Cruz Biotechnology; sc-32725, 1:2000) at 4°C overnight. Then, they were incubated with secondary antibody (Invitrogen, USA) for 1 h. DAPI was applied for dyeing nucleus. In the end, the fluorescence microscope (Nikon, Japan) was applied for analysis.

2.6. Immunohistochemistry (IHC)

The paraffin-embedded brain sections were quenched to inactivate endogenous peroxidase for half an hour utilizing 0.5% H₂O₂. After blocking with 5% goat serum, sections were incubated with primary antibody against TNFRSF6 (Santa Cruz Biotechnology) at 4°C overnight. Next, sections were rinsed and cultured with secondary antibody for 1 h, followed by visualizing through the DAB kit (Beyotime). A light microscope (Nikon) was applied

for observation.

2.7. Western blot

Hippocampus tissues and microglia were homogenized in RIPA lysis buffer (Beyotime Biotechnology, China) and subjected to centrifugation. Protein samples were separated on 10% SDS-PAGE and then transferred onto PVDF membranes. Membranes were blocked and incubated with primary antibodies against TNFRSF6 (Santa Cruz Biotechnology, USA, sc-74540, 1:2000) and GAPDH (Abcam, ab8245, 1:2500) at 4°C for a whole night, followed by incubating with secondary antibody (Abcam, ab205718, 1:2000) for 1 h. The proteins were visualized and analyzed by ECL reagents and Image J.

2.8. RT-qPCR

Total RNA was isolated utilizing TRIzol Kit (Omega, Norcross, GA, USA). Then, cDNA was synthesized by the cDNA Synthesis Kit (Takara, Japan). qPCR was conducted by SYBR Green PCR Master Mix (Takara) on a StepOnePlus RT-qPCR system. Gene expression was estimated by the $2^{-\Delta\Delta C_t}$ method normalized to GAPDH.

2.9. ELISA

In accordance with the user guides of the corresponding ELISA kit (Beijing 4A Biotech Co., Ltd), IL-1 β , IL-6, TNF- α , and IL-10 concentrations were determined in the supernatant of microglia and hippocampus tissues. The microplate reader (BioTek, USA) was applied to measure the absorbance at 450 nm.

2.10. ATP content detection

Based on the user guides, ATP content was tested through the ATP Solarbio Life Sciences Assay kit. The supernatant of brain tissues was subjected to centrifugation at 1000 g 4°C for 10 min, followed by transferring to the EP tube. Next, ATP content was assessed in the homogenized lysates utilizing a microplate reader (BioTek, USA).

2.11. DCFHDA assay

ROS levels were assessed in hippocampus tissues and microglia utilizing the ROS-specific fluorescent probe (Applygen Technologies Inc.) and dichlorodihydrofluorescein diacetate (DCFHDA). The microplate reader (BioTek, USA) was utilized for measuring the fluorescence intensity.

2.12. JC-1 assay

Mitochondrial membrane potential (MMP) was tested utilizing the JC-1 dye (Beyotime) in accordance with user guides. Mitochondrion was subjected to isolation from tissues utilizing a Tissue Mitochondrial isolation kit (Beyotime). Then the isolated mitochondrion was stained with JC-1 solution for half an hour. When the MMP level is high, the fluorescence properties change from green to red.

2.13. Detection of mitochondrial function

Mitochondrial oxygen consumption in hippocampus samples was tested utilizing O2k- Fluorespirometer [19] (OROBOROS INSTRUMENTS, Austria). The hippocampus was dissected, weighed, cut into small pieces with scissors, and then homogenized. The procedures were implemented under sustained stirring in the Mir05 respiration medium. After reaching the stable baseline

respiration, LEAK respiration was assessed after complex specific substrate oxidation. The maximum oxidative phosphorylation capacity (OXPHOS) was determined via saturating ADP concentration (2.5 mM). ROS production was suppressed via rotenone before succinate supplement. ATP was suppressed via oligomycin to assess LEAK respiration in a non-phosphorylating state. The respiratory control ratio (RCR) was expressed as the rate of OXPHOS to LEAK. The DatLab software (OROBOROS) was employed for analysis.

2.14. Statistical analysis

Statistical analyses were performed by the application of GraphPad Prism 8 software. The group difference was analyzed with student's t-test or one-way ANOVA. Data are presented as mean \pm SD from 3 individual repeats. $p < 0.05$ was considered significant.

3. Results

3.1. TNFRSF6 is upregulated in the LPS-induced septic model *in vivo* and *in vitro*

For the sake of selecting genes that may play a regulatory role in SAE, we used the GSE167610 and GSE171696 datasets. After taking the intersection of these two datasets, we obtained the unique intersection TNFRSF6 (Figure 1A). Further analysis of the dataset illustrated that

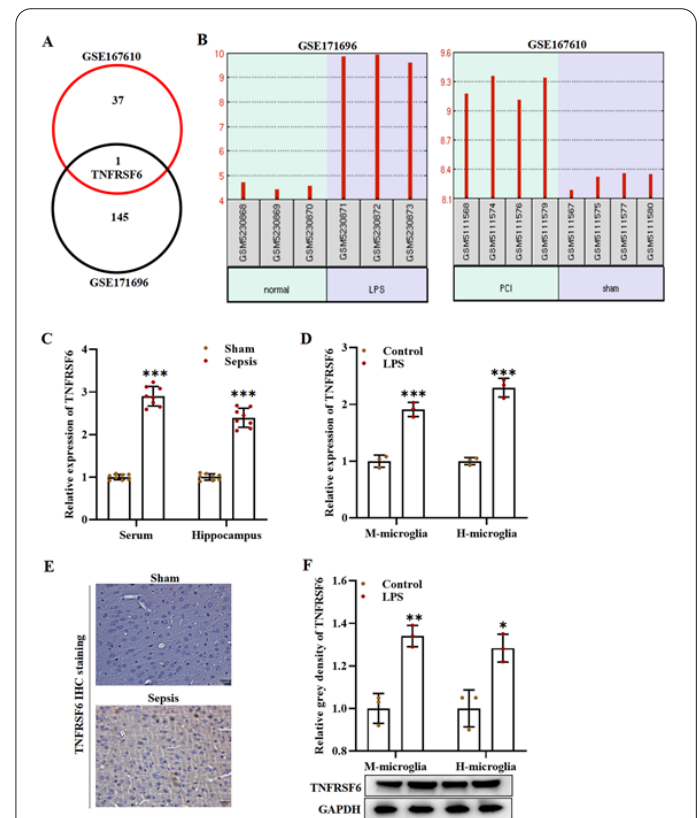


Fig. 1. TNFRSF6 is upregulated in LPS-induced sepsis models *in vivo* and *in vitro*. (A) TNFRSF6 was screened through the intersection of GSE167610 and GSE171696 datasets. (B) TNFRSF6 expression in normal cells and LPS-induced cells, as well as the sham tissues and peritoneal contamination and infection (PCI) tissues. (C-D) RT-qPCR showing TNFRSF6 expression in the serum and hippocampus of sham and sepsis mice as well as the M-microglia and H-microglia of control and LPS groups. (E) IHC staining of TNFRSF6 in hippocampal samples of sham mice or sepsis mice. (F) Western blot analysis of TNFRSF6 protein levels in M-microglia and H-microglia of the control and LPS group. * $p < 0.05$, ** $p < 0.01$, *** $p < 0.001$.

TNFRSF6 expression was increased in both the LPS-induced BV-2 microglia and SAE mouse model (Figure 1B). Therefore, TNFRSF6 was deeply explored as our research object. LPS was utilized for constructing mouse and cell models of SAE. Next, we examined TNFRSF6 expression in both *in vivo* and *in vitro* models. RT-qPCR outcomes manifested that TNFRSF6 expression was notably upregulated in the serum and hippocampus of septic mice in comparison to the sham mice (Figure 1C). Similarly, we also observed overexpression of TNFRSF6 in LPS-induced mouse microglia (M-microglia) and human microglia (H-microglia) (Figure 1D). Then, by IHC staining of hippocampus samples, we discovered that TNFRSF6 expression was increased in LPS-induced sepsis mice (Figure 1E). Further analysis of western blot manifested that TNFRSF6 exhibited high protein levels in LPS-induced M-microglia and H-microglia (Figure 1F). Thus, we confirmed that TNFRSF6 was upregulated in the LPS-induced septic model *in vivo* and *in vitro*.

3.2. TNFRSF6 deficiency attenuates sepsis-impaired learning, memory and cognitive functions in mice

For further investigating the function of TNFRSF6 on SAE, we purchased the TNFRSF6 knockout (TNFRSF6^{-/-}) mice and then treated them with LPS for modeling. Western blot outcomes displayed that TNFRSF6 protein levels were increased in the LPS-induced WT septic mice while reducing in the LPS-induced TNFRSF6^{-/-} septic mice (Figure 2A). Then, we performed the behavior tests for measuring the impacts of TNFRSF6 on learning, memory and cognitive functions in sepsis mice. Barnes maze tests showed that, in comparison of the corresponding sham mice, both WT and TNFRSF6^{-/-} sepsis mice possessed a longer time to recognize target boxes. However, in comparison to WT sepsis mice, it took a shorter time for TNFRSF6^{-/-} sepsis mice to recognize target boxes (Figure 2B). Next, we found that LPS treatment decreased the freezing time in the context and tone-related fear conditioning of sepsis mice, while TNFRSF6 depletion elevated the freezing time of sepsis mice (Figure 2C-D). Collectively, TNFRSF6 deficiency alleviated sepsis-induced learning and memory impairments. Furthermore, we discovered that lower recognition index (Figure 2E) and less time in the target quadrant and across platforms (Figure 2F) in sepsis mice, while TNFRSF6 deficiency improved these behaviors. Thus, we confirmed that TNFRSF6 deficiency alleviated the impaired learning, memory and cognitive functions in SAE mice.

3.3. TNFRSF6 deficiency alleviates neuronal injury, microglial activation, and inflammation in the mouse model of SAE

We then obtained the hippocampus tissues from SAE mice and evaluated the impacts of TNFRSF6 deficiency on neuronal injury. Nissl staining of hippocampus tissues showed copious purple nuclei and abundant Nissl bodies in neurons of sham mice. However, in the hippocampus of WT sepsis mice, we observed an increase in neuronal loss and Nissl body deficiency, indicating that LPS induction increased neuronal damage in sepsis mice. Compared with the WT sepsis mice, we found that neuronal loss was reduced and the quantity of Nissl body was elevated in the TNFRSF6^{-/-} sepsis mice, suggesting TNFRSF6 deficiency alleviated neuronal injury in the hippocampus

(Figure 3A). Then, IF results illustrated that the quantity of Iba-1-positive cells was notably increased in WT sepsis

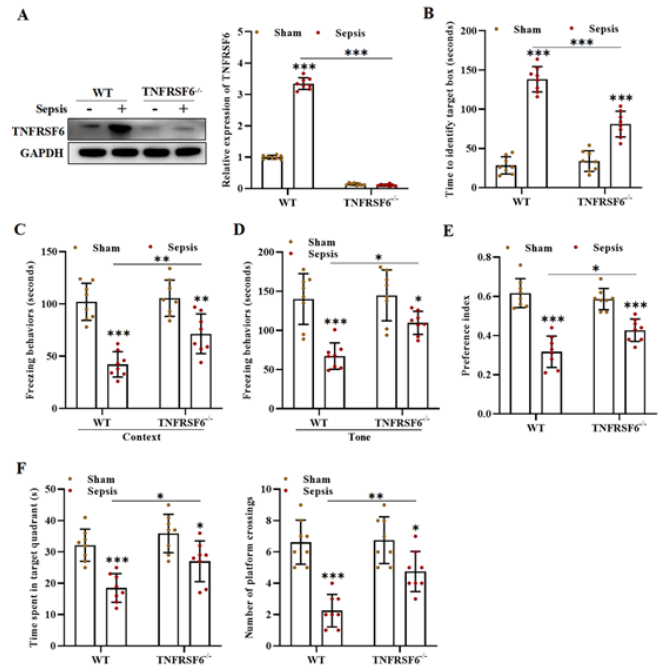


Fig. 2. TNFRSF6 deficiency attenuates learning, memory and cognitive functions in SAE mice. (A) Western blot outcomes of TNFRSF6 protein levels in hippocampal samples of the sham-WT, sepsis-WT, sham-TNFRSF6^{-/-}, and sepsis-TNFRSF6^{-/-} mice. (B-F) Behavioral assessment of mice using Barnes maze (B), context or tone-related fear conditioning test (C-D), novel object recognition test (E), and MWM test (F). **p*<0.05, ***p*<0.01, ****p*<0.001.

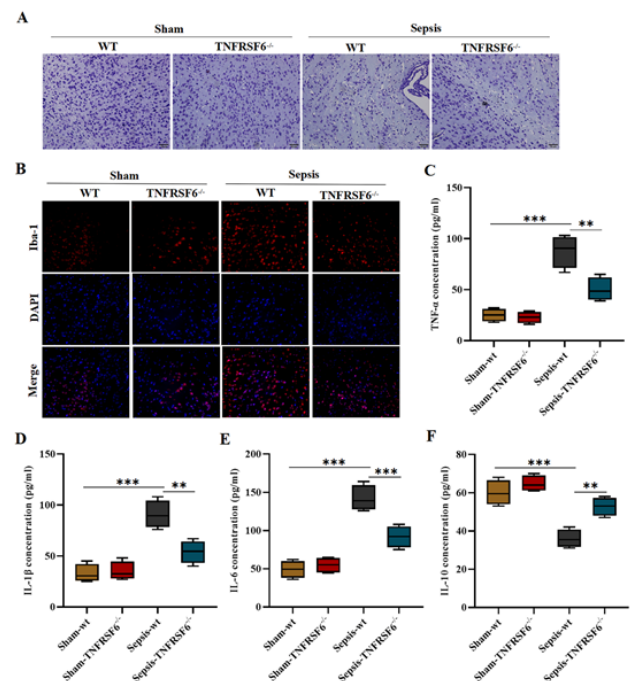


Fig. 3. TNFRSF6 deficiency alleviates neuronal injury, microglial activation, and inflammation in SAE mouse models. (A) Nissl staining of hippocampal tissues in sham-WT mice, sham-TNFRSF6^{-/-} mice, sepsis-WT mice, and sepsis-TNFRSF6^{-/-} mice to evaluate neuronal injury. (B) Quantification of Iba-1-positive cells using IF in different groups. (C-F) ELISA results of TNF-α, IL-1β, IL-6, and IL-10 concentrations in different hippocampal samples. ***p*<0.01, ****p*<0.001.

mice in comparison of sham mice, while it was reduced in TNFRSF6^{-/-} sepsis mice, suggesting TNFRSF6 deficiency could suppress microglial activation (Figure 3B). Then, it was manifested by ELISA that the contents of proinflammatory factors TNF- α , IL-1 β , and IL-6 were markedly elevated in sepsis-WT group compared with sham groups while reducing in the sepsis-TNFRSF6^{-/-} group compared with sepsis-WT group (Figure 3C-E). The contents of anti-inflammatory factor IL-10 exhibited the opposite trend (Figure 3F). Overall, we confirmed that TNFRSF6 deficiency alleviated neuronal injury, microglial activation, and inflammation in SAE mice.

3.4. TNFRSF6 deficiency improves mitochondrial dysfunction in septic mice

The alterations in mitochondrial dysfunction in the septic mice were investigated. After the onset of sepsis, we found that hippocampal complex I-linked respirations were suppressed because of the decline (LEAK_{GM}, OXPHOS and RCR, while TNFRSF6 depletion reversed these indexes (Figure 4A). Similarly, hippocampal complex II-dependent respirations were inhibited by sepsis, and the suppressed LEAK_{GM} and OXPHOS could be recovered by TNFRSF6 deficiency; however, RCR did not show significant alterations in the sham group, sepsis group, or TNFRSF6 depletion group (Figure 4A). Furthermore, ATP content, mtROS, and MMP were evaluated for evaluating mitochondrial function in hippocampus tissues. The outcomes manifested that, in comparison of sham-WT and sham-TNFRSF6^{-/-} groups, ATP content was notably declined in sepsis-WT group, while partly reversed in sepsis-TNFRSF6^{-/-} group (Figure 4B). By contraries, DCFH-DA assay manifested that mtROS value was increased in sepsis-WT mice, but sepsis-TNFRSF6^{-/-} mice showed a notable declination in mtROS (Figure 4C). Additionally, JC-1 assay illustrated that, compared with sham groups, JC-1 aggregate was elevated in sepsis-WT group and reduced in sepsis-TNFRSF6^{-/-} group, demonstrating that MMP damage increased in sepsis could be recovered by TNFRSF6 depletion (Figure 4D). These results confirmed that TNFRSF6 deficiency improved mitochondrial dysfunction in the septic mice.

3.5. TNFRSF6 deficiency reduces inflammatory response and alleviates mitochondrial dysfunction in LPS-stimulated microglia

In the end, we evaluated the impacts of TNFRSF6 on SAE process through the *in vitro* cell assays. M-microglia and H-microglia were treated with LPS for modeling and transfected with shTNFRSF6 for silencing TNFRSF6 in cells. Through ELISA, we observed that TNF- α , IL-1 β , and IL-6 contents markedly elevated via LPS induction were reduced by TNFRSF6 knockdown, while IL-10 showed the opposite trend (Figure 5A-D). DCFH-DA assay further demonstrated that LPS stimulation notably enhanced ROS release in M-microglia and H-microglia, while TNFRSF6 deficiency abolished the function of LPS (Figure 5E). ATP contents in M-microglia and H-microglia decreased by LPS stimulation could be recovered by TNFRSF6 downregulation (Figure 5F). Additionally, MMP damage strengthened by LPS stimulation could be reversed by TNFRSF6 depletion (Figure 5G). Thus, we proved that TNFRSF6 deficiency reduced inflammatory response and alleviated mitochondrial dysfunction in

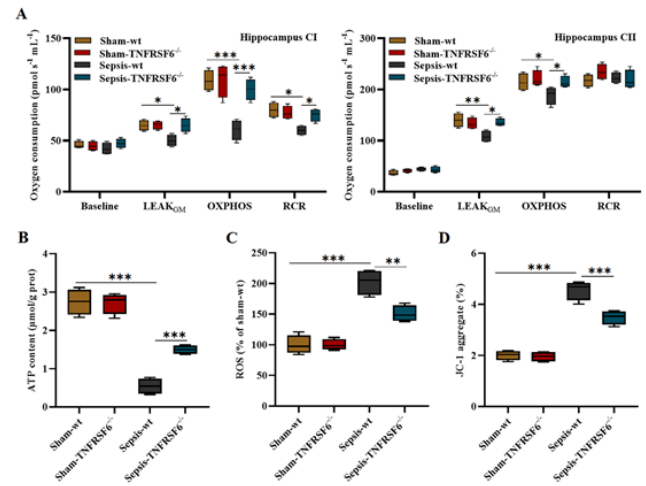


Fig. 4. NFRSF6 deficiency improves mitochondrial dysfunction in septic mice. (A) Hippocampus complex I/II-linked mitochondrial oxygen consumption in sham-WT, sham-TNFRSF6^{-/-}, sepsis-WT, and sepsis-TNFRSF6^{-/-} mice. (B) Determination of ATP content in different hippocampal tissues. (C) mtROS production estimated using DCFH-DA assay. (D) MMP loss determined using JC-1 assay. **p*<0.05, ***p*<0.01, ****p*<0.001.

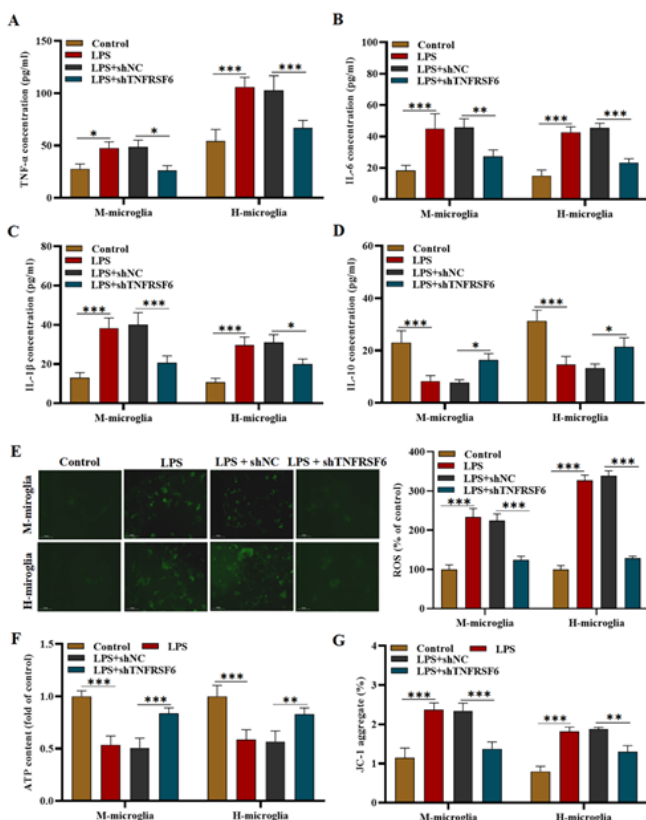


Fig. 5. TNFRSF6 deficiency reduces inflammatory response and alleviates mitochondrial dysfunction in LPS-stimulated microglia. (A-D) ELISA results of TNF- α , IL-1 β , IL-6, and IL-10 concentrations in M-microglia and H-microglia of control, LPS, LPS+shNC, and LPS+shTNFRSF6 groups. (E) ROS production estimated using DCFH-DA assay. (F) Assessment of ATP level in different cells. (G) MMP loss determined using JC-1 assay. **p*<0.05, ***p*<0.01, ****p*<0.001.

LPS-stimulated microglia.

4. Discussion

SAE is the main complication of sepsis, accompa-

nied by irreversible brain damage, which seriously affects the quality of life of patients. Therefore, revealing the pathogenesis of SAE is of great significance. Microglia activation is critical to neuroinflammation and SAE development [20, 21]. At present, some studies have revealed that the inhibition of microglia activation can alleviate the SAE process. For example, SIRT3 depletion can inhibit LPS-induced microglial activation and inflammatory cytokine to alleviate SAE progression [22]. TNFRSF6 is a member of the TNFR superfamily and exerts the regulatory function in immune system diseases [16, 23]. Studies have confirmed that TNF is related to blood-brain barrier destruction, astrocyte activation, and neuronal apoptosis, and these phenomena do not appear in mice with TNFR deficiency [24]. Furthermore, TNFR is confirmed to be negatively correlated with memory capability in animal models [25]. In this study, we used LPS to induce a mouse model of SAE. LPS-induced mouse model of sepsis shows the reduced proliferation of new neurons and dysfunction differentiation in the dentate gyrus. Additionally, LPS has been confirmed to strongly stimulate the activation of microglia, and the disordered activation of microglia can aggravate brain tissue damage during SAE. Therefore, we used LPS-induced microglia as the SAE cell injury model. In this study, we found that TNFRSF6 was significantly overexpressed in the serum and hippocampus of SAE mice. At the same time, high expression of TNFRSF6 was also observed in LPS-induced human microglia and mouse microglia. Next, we used TNFRSF6 knockout mice to construct an SAE mouse model and conducted behavioral tests on the mice. We found that the learning, memory, and cognitive functions of SAE mice were severely damaged, but the knockout of TNFRSF6 significantly alleviated sepsis-induced damages and restored the behavioral function of the mice. Therefore, we believe that TNFRSF6 is involved in regulating the progress of SAE.

Neuroinflammation exerts a vital function in SAE pathogenesis [26]. Neuroinflammation refers to inflammation in CNS, characterized by the activation of microglia, the increase of inflammatory factors and the recruitment of white blood cells, which ultimately leads to neuronal damage. In the early stage of sepsis, microglia are activated and transformed into M1 proinflammatory phenotype, resulting in the secretion of inflammatory cytokines, such as IL-1 β , IL-6 and TNF- α in brain, further aggravating neuroinflammation [27, 28]. Recent studies have confirmed that inhibition of microglia activation and inflammatory response may partially reverse cognitive impairment caused by SAE [8]. Therefore, the modulation on the activation of microglia and the subsequent inflammatory response is crucial for controlling SAE. Herein, we observed that the induction of sepsis promoted microglia activation and increased the loss of neurons in the hippocampus of SAE mice. In addition, IL-1 β , IL-6 and TNF- α levels were notably elevated in SAE mice and LPS-induced microglia. However, TNFRSF6 knockout significantly reduced their levels. At the same time, the level of anti-inflammatory factor IL-10 inhibited by sepsis effectively rebounded after TNFRSF6 knockdown. These results provide evidence for the key role of microglia-mediated neuroinflammation in SAE. Therefore, we believe that TNFRSF6 promotes microglia activation and neuroinflammation in SAE.

Studies have shown that oxidative stress and inflammatory response in the brain of SAE rats may lead to mi-

tochondrial dysfunction [29]. Mitochondria are the intracellular organelles that exert crucial function in cells via synthesizing ATP via respiration and oxidative phosphorylation (OXPHOS) [30]. In SAE, LPS induction leads to the loss of MMP, which then initiates the cell death pathway. Furthermore, mitochondria are the main source of ROS that may lead to intracellular oxidative stress [31]. Research has shown that ROS overproduction during sepsis can exacerbate mitochondrial injury and reduce ATP content, leading to cell metabolism deficiency and bioenergy depletion [32, 33]. ATP is an effective central link between energy generation and energy demand processes. Evidence shows a decrease in ATP concentration in non-survivors of sepsis patients [34]. Herein, we proved that brain mitochondria were damaged by LPS-induced sepsis, as evidenced by the reduction in the substrate LEAKGM and OXPHOS in hippocampal tissues. Furthermore, we observed the decrease of ATP content and the increase of ROS production and MMP loss in LPS-induced SAE mice and microglia. ROS overproduction caused via LPS caused mitochondrial dysfunction and inhibited mitochondrial respiratory chain complexes. The injured mitochondria further impaired their capability to produce ATP. These discoveries supported the previous study on a declination in mitochondrial activity (complex I) and an enhancement on ROS release in sepsis animal model [35]. However, TNFRSF6 depletion reversed these indexes to improve mitochondrial disorder. Thus, we confirm that TNFRSF6 deficiency improves mitochondrial dysfunction in SAE.

Taken together, this study proves that TNFRSF6 induces microglia activation and mitochondrial dysfunction in SAE. Our study confirms for the first time that TNFRSF6 functions in SAE, which may provide new therapeutic targets for SAE.

Informed consent

The authors report no conflict of interest.

Availability of data and material

We declared that we embedded all data in the manuscript.

Authors' contributions

YD, JY and ZJ conducted the experiments and wrote the paper; YD and HX conceived, designed the study and revised the manuscript.

Funding

None.

Acknowledgements

We thanked Taihe Hospital, Hubei University of Medicine for approving our study.

References

1. Singer M, Deutschman CS, Seymour CW, Shankar-Hari M, Annane D, Bauer M, Bellomo R, Bernard GR, Chiche JD, Cooper-Smith CM, Hotchkiss RS, Levy MM, Marshall JC, Martin GS, Opal SM, Rubenfeld GD, van der Poll T, Vincent JL, Angus DC (2016) The Third International Consensus Definitions for Sepsis and Septic Shock (Sepsis-3). *Jama* 315 (8): 801-810. doi: 10.1001/jama.2016.0287
2. Salomão R, Ferreira BL, Salomão MC, Santos SS, Azevedo LCP, Brunialti MKC (2019) Sepsis: evolving concepts and challenges. *Braz J Med Biol Res* 52 (4): e8595. doi: 10.1590/1414-431x20198595
3. Sprung CL, Peduzzi PN, Shatney CH, Schein RM, Wilson MF, Sheagren JN, Hinshaw LB (1990) Impact of encephalopathy on

- mortality in the sepsis syndrome. The Veterans Administration Systemic Sepsis Cooperative Study Group. *Crit Care Med* 18 (8): 801-806. doi: 10.1097/00003246-199008000-00001
4. Chung HY, Wickel J, Brunkhorst FM, Geis C (2020) Sepsis-Associated Encephalopathy: From Delirium to Dementia? *J Clin Med* 9 (3). doi: 10.3390/jcm9030703
 5. Gao Q, Hernandez MS (2021) Sepsis-Associated Encephalopathy and Blood-Brain Barrier Dysfunction. *Inflammation* 44 (6): 2143-2150. doi: 10.1007/s10753-021-01501-3
 6. Zhao L, Gao Y, Guo S, Lu X, Yu S, Ge ZZ, Zhu HD, Li Y (2021) Sepsis-Associated Encephalopathy: Insight into Injury and Pathogenesis. *CNS Neurol Disord Drug Targets* 20 (2): 112-124. doi: 10.2174/1871527319999201117122158
 7. Yan X, Yang K, Xiao Q, Hou R, Pan X, Zhu X (2022) Central role of microglia in sepsis-associated encephalopathy: From mechanism to therapy. *Front Immunol* 13: 929316. doi: 10.3389/fimmu.2022.929316
 8. Li Y, Yin L, Fan Z, Su B, Chen Y, Ma Y, Zhong Y, Hou W, Fang Z, Zhang X (2020) Microglia: A Potential Therapeutic Target for Sepsis-Associated Encephalopathy and Sepsis-Associated Chronic Pain. *Front Pharmacol* 11: 600421. doi: 10.3389/fphar.2020.600421
 9. Kanakdande AP and Jadhav PB (2023). Anti-urinary tract infection activity of selected herbal extract towards isolated *Kosakonia cowanii* (OQ 073698). *Cell Mol Biomed Rep* 3(2):114-121. doi: <https://doi.org/10.55705/cnbr.2023.385428.1099>
 10. Subhramanyam CS, Wang C, Hu Q, Dheen ST (2019) Microglia-mediated neuroinflammation in neurodegenerative diseases. *Semin Cell Dev Biol* 94: 112-120. doi: 10.1016/j.semcdb.2019.05.004
 11. Kwon HS, Koh SH (2020) Neuroinflammation in neurodegenerative disorders: the roles of microglia and astrocytes. *Transl Neurodegener* 9 (1): 42. doi: 10.1186/s40035-020-00221-2
 12. Yang L, Li Z, Xu Z, Zhang B, Liu A, He Q, Zheng F, Zhan J (2022) Protective Effects of Cannabinoid Type 2 Receptor Activation Against Microglia Overactivation and Neuronal Pyroptosis in Sepsis-Associated Encephalopathy. *Neuroscience* 493: 99-108. doi: 10.1016/j.neuroscience.2022.04.011
 13. Peng LS, Xu Y, Wang QS (2022) YY1 PROMOTES MICROGLIA M2 POLARIZATION THROUGH THE MIR-130A-3P/TREM-2 AXIS TO ALLEVIATE SEPSIS-ASSOCIATED ENCEPHALOPATHY. *Shock* 58 (2): 128-136. doi: 10.1097/shk.0000000000001914
 14. Sziller I, Hupuczsi P, Normand N, Halmos A, Papp Z, Witkin SS (2006) Fas (TNFRSF6) gene polymorphism in pregnant women with hemolysis, elevated liver enzymes, and low platelets and in their neonates. *Obstet Gynecol* 107 (3): 582-587. doi: 10.1097/01.Aog.0000195824.51919.81
 15. Savinov AY, Tcherepanov A, Green EA, Flavell RA, Chervonsky AV (2003) Contribution of Fas to diabetes development. *Proc Natl Acad Sci U S A* 100 (2): 628-632. doi: 10.1073/pnas.0237359100
 16. Feuk L, Prince JA, Breen G, Emahazion T, Carothers A, St Clair D, Brookes AJ (2000) apolipoprotein-E dependent role for the FAS receptor in early onset Alzheimer's disease: finding of a positive association for a polymorphism in the TNFRSF6 gene. *Hum Genet* 107 (4): 391-396. doi: 10.1007/s004390000383
 17. Pan C, Si Y, Meng Q, Jing L, Chen L, Zhang Y, Bao H (2019) Suppression of the RAC1/MLK3/p38 Signaling Pathway by β -Elemene Alleviates Sepsis-Associated Encephalopathy in Mice. *Front Neurosci* 13: 358. doi: 10.3389/fnins.2019.00358
 18. Liang P, Shan W, Zuo Z (2018) Perioperative use of cefazolin ameliorates postoperative cognitive dysfunction but induces gut inflammation in mice. *J Neuroinflammation* 15 (1): 235. doi: 10.1186/s12974-018-1274-6
 19. Juhász L, Rutai A, Fejes R, Tallósy SP, Poles MZ, Szabó A, Szatmári I, Fülöp F, Vécsei L, Boros M, Kaszaki J (2020) Divergent Effects of the N-Methyl-D-Aspartate Receptor Antagonist Kynurenic Acid and the Synthetic Analog SZR-72 on Microcirculatory and Mitochondrial Dysfunction in Experimental Sepsis. *Front Med (Lausanne)* 7: 566582. doi: 10.3389/fmed.2020.566582
 20. Woodburn SC, Bollinger JL, Wohleb ES (2021) The semantics of microglia activation: neuroinflammation, homeostasis, and stress. *J Neuroinflammation* 18 (1): 258. doi: 10.1186/s12974-021-02309-6
 21. Castro LVG, Gonçalves-de-Albuquerque CF, Silva AR (2022) Polarization of Microglia and Its Therapeutic Potential in Sepsis. *Int J Mol Sci* 23 (9). doi: 10.3390/ijms23094925
 22. He C, Aziguli A, Zhen J, Jiao A, Liao H, Du C, Liu W, Aihemaitijiang K, Xu A (2022) MiRNA-494 specifically inhibits SIRT3-mediated microglia activation in sepsis-associated encephalopathy. *Transl Cancer Res* 11 (7): 2299-2309. doi: 10.21037/tcr-22-1732
 23. Neven B, Magerus-Chatinet A, Florquin B, Gobert D, Lambotte O, De Somer L, Lanzarotti N, Stolzenberg MC, Bader-Meunier B, Aladjidi N, Chantrain C, Bertrand Y, Jeziorski E, Leverger G, Michel G, Suarez F, Oksenhendler E, Hermine O, Blanche S, Picard C, Fischer A, Rieux-Laucat F (2011) A survey of 90 patients with autoimmune lymphoproliferative syndrome related to TNFRSF6 mutation. *Blood* 118 (18): 4798-4807. doi: 10.1182/blood-2011-04-347641
 24. Alexander JJ, Jacob A, Cunningham P, Hensley L, Quigg RJ (2008) TNF is a key mediator of septic encephalopathy acting through its receptor, TNF receptor-1. *Neurochem Int* 52 (3): 447-456. doi: 10.1016/j.neuint.2007.08.006
 25. Krabbe KS, Reichenberg A, Yirmiya R, Smed A, Pedersen BK, Bruunsgaard H (2005) Low-dose endotoxemia and human neuropsychological functions. *Brain Behav Immun* 19 (5): 453-460. doi: 10.1016/j.bbi.2005.04.010
 26. Pan S, Lv Z, Wang R, Shu H, Yuan S, Yu Y, Shang Y (2022) Sepsis-Induced Brain Dysfunction: Pathogenesis, Diagnosis, and Treatment. *Oxid Med Cell Longev* 2022: 1328729. doi: 10.1155/2022/1328729
 27. Liu X, Zhang M, Liu H, Zhu R, He H, Zhou Y, Zhang Y, Li C, Liang D, Zeng Q, Huang G (2021) Bone marrow mesenchymal stem cell-derived exosomes attenuate cerebral ischemia-reperfusion injury-induced neuroinflammation and pyroptosis by modulating microglia M1/M2 phenotypes. *Exp Neurol* 341: 113700. doi: 10.1016/j.expneurol.2021.113700
 28. Yang X, Xu S, Qian Y, Xiao Q (2017) Resveratrol regulates microglia M1/M2 polarization via PGC-1 α in conditions of neuroinflammatory injury. *Brain Behav Immun* 64: 162-172. doi: 10.1016/j.bbi.2017.03.003
 29. Zhang X, Ji R, Liao X, Castellero E, Kennel PJ, Brunjes DL, Franz M, Möbius-Winkler S, Drosatos K, George I, Chen EI, Colombo PC, Schulze PC (2018) MicroRNA-195 Regulates Metabolism in Failing Myocardium Via Alterations in Sirtuin 3 Expression and Mitochondrial Protein Acetylation. *Circulation* 137 (19): 2052-2067. doi: 10.1161/circulationaha.117.030486
 30. Nunnari J, Suomalainen A (2012) Mitochondria: in sickness and in health. *Cell* 148 (6): 1145-1159. doi: 10.1016/j.cell.2012.02.035
 31. Yang Y, Karakhanova S, Hartwig W, D'Haese JG, Philippov PP, Werner J, Bazhin AV (2016) Mitochondria and Mitochondrial ROS in Cancer: Novel Targets for Anticancer Therapy. *J Cell Physiol* 231 (12): 2570-2581. doi: 10.1002/jcp.25349
 32. Stefanatos R, Sanz A (2018) The role of mitochondrial ROS in the aging brain. *FEBS Lett* 592 (5): 743-758. doi: 10.1002/1873-3468.12902
 33. van Hameren G, Campbell G, Deck M, Berthelot J, Gautier B,

- Quintana P, Chrast R, Tricaud N (2019) In vivo real-time dynamics of ATP and ROS production in axonal mitochondria show decoupling in mouse models of peripheral neuropathies. *Acta Neuropathol Commun* 7 (1): 86. doi: 10.1186/s40478-019-0740-4
34. Brealey D, Brand M, Hargreaves I, Heales S, Land J, Smolenski R, Davies NA, Cooper CE, Singer M (2002) Association between mitochondrial dysfunction and severity and outcome of septic shock. *Lancet* 360 (9328): 219-223. doi: 10.1016/s0140-6736(02)09459-x
35. Comim CM, Rezin GT, Scaini G, Di-Pietro PB, Cardoso MR, Petronilho FC, Ritter C, Streck EL, Quevedo J, Dal-Pizzol F (2008) Mitochondrial respiratory chain and creatine kinase activities in rat brain after sepsis induced by cecal ligation and perforation. *Mitochondrion* 8 (4): 313-318. doi: 10.1016/j.mito.2008.07.002